VU VRIJE UNIVERSITEIT AMSTERDAM

VU Research Portal

Implementation, Calculation and Interpretation of Vibrational Circular Dichroism Spectra

Nicu, V.P.

2009

document version
Publisher's PDF, also known as Version of record

Link to publication in VU Research Portal

citation for published version (APA)
Nicu, V. P. (2009). *Implementation, Calculation and Interpretation of Vibrational Circular Dichroism Spectra*. [PhD-Thesis - Research and graduation internal, Vrije Universiteit Amsterdam].

General rights
Copyright and moral rights for the publications made accessible in the public portal are retained by the authors and/or other copyright owners and it is a condition of accessing publications that users recognise and abide by the legal requirements associated with these rights.

- Users may download and print one copy of any publication from the public portal for the purpose of private study or research.
- You may not further distribute the material or use it for any profit-making activity or commercial gain
- You may freely distribute the URL identifying the publication in the public portal ?

Take down policy
If you believe that this document breaches copyright please contact us providing details, and we will remove access to the work immediately and investigate your claim.

E-mail address:
vuresearchportal.ub@vu.nl

Download date: 05. May. 2023

Chapter 5

Robust Normal Modes in VCD Spectra

5.1 Introduction

When using VCD, the AC of a given molecule is determined by comparing its experimental and calculated VCD spectra. The procedure relies on two facts, the optical enantiomers have VCD spectra of equal magnitude but opposite sign, and the AC of the molecule used in the calculation is known. Therefore, in order to have reliable prediction of AC using VCD, accurate calculations of VCD spectra are required.

Very good agreement between experimental and calculated VCD spectra [50, 54, 81–83] is obtained when the effects induced by the solvent are negligible and when the calculation is for the conformation present in solution (i.e. in case of rigid molecules, or in general if a single conformation is populated in the experimental sample). However, very often these conditions are not met. Many studies [66, 72, 84–88] have shown that the shapes of VCD spectra depend sensitively on the solvent used and also on the concentration of the solute. At the same time, perturbations such as solute-solvent and/or solute-solute interactions are neglected in calculations performed on isolated gas phase molecules. Thus, discrepancies between calculated VCD spectra and experimental VCD spectra measured in solution are often observed.

Currently, continuum solvation models [89] are the only methodology available for modeling solvent effects in DFT VCD calculations. However, as a number of studies have shown [61, 66–68, 70–72, 85] approximating the solvent by a continuum dielectric medium is not sufficient to model the effects on the VCD spectra; specific interactions such as hydrogen-bonding must be taken into account.

Therefore, until more accurate treatments of the solvent will be available, it is desirable to know: a) what type of discrepancies between calculated gas phase VCD spectra and solution experimental VCD spectra can be ascribed to solvent effects, b) what are the mechanisms that induce the observed discrepancies, and c) which of the normal modes are likely/unlikely to be affected by the solvent.

We have addressed these questions in the previous chapter by investigating (theoretically) the effects induced in the VCD spectra by complex formation. As shown in chapter 4, the various differences observed when comparing experimental and calculated VCD spectra (e.g modes that have different signs, modes with significantly different VCD intensities, modes with shifted frequencies, the appearance of new VCD signals) can all be encountered in case of, and can be explained by complex formation. The theoretical analysis in chapter 4 of the mechanisms that induce the effects enumerated above has shown that: A) some normal modes are more susceptible than others to exhibit a sign change of their rotational strength, and B) the same mechanisms can induce either a change of sign or a change of magnitude of the rotational strengths. These findings led us to the conclusion that the normal modes in a VCD spectrum can be classified as *robust* and *non-robust*. The sign of the rotational strengths of the *non-robust* modes can easily be changed by small perturbations (e.g. solvent effects). The *robust* modes on the other hand have rotational strengths with characteristic sign that should not be affected by small perturbations.

As discussed in the previous chapters, VCD intensities are determined by the rotational strengths (R). Depending on the value of the angle $\xi(i)$ between the vectors electric and magnetic dipole transition moments (EDTM and MDTM) of a mode i, the $R(i)$ can be positive or negative. Thus, $R(i)$ is positive when the angle $\xi(i)$ is smaller than 90° since $\cos[\xi(i)] > 0$, whereas when $\xi(i)$ is larger than 90° $R(i)$ is negative since $\cos[\xi(i)] < 0$. However, when $\xi(i)$ is close to 90°, even a small perturbation can change $\xi(i)$ across 90°. This will result in a sign change. Thus, the *non-robust* modes are characterized by values of ξ that are close to 90°, and as a result their sign can be changed easily. The *robust modes* on the other hand, have ξ angles that are far from 90° and therefore their sign is less likely to be changed by small perturbations present in the experiment or when using slightly different computational parameters.

At the computational side, the choice of exchange-correlation functional affects the calculated VCD spectra. There are many reasonable functionals, and there has not yet emerged one that is clearly universally superior. Moreover, combined experimental and computational studies by Stephens et al. [90, 91] have shown that in case of VCD, in order to achieve good agreement between experimental and calculated spectra, the exchange-correlation functional is the

most critical computational parameter. Therefore, going from one functional to another one may be considered a computational perturbation.

In this chapter we investigate this computational perturbation in the light of the distinction between robust and non-robust modes. There are two questions that need to be answered: 1) Can we apply this concept also to this type of perturbation, and 2) can we identify the modes that can safely be used in the comparison between experiment and theory to distinguish between different ACs? Answering these question should tell us which modes should be used (or not used) when determining the AC of a compound using VCD. There are always discrepancies between experiment and theory in the sign and magnitude of some rotational strengths, but when they are for non-robust modes, they should be of no concern.

The goal of this study is to establish criteria for determining the robustness of the normal modes in the calculated VCD spectra, i.e to determine an appropriate angle interval that enables one to classify a normal mode i as *robust* or *non-robust* depending whether or not its angle $\xi(i)$ belongs to that angle interval. To achieve this, we investigate: 1) the range of values taken by the ξ angles of the normal modes of various molecules, and 2) how the values of the ξ angles change when different exchange-correlation (BP86 vs. OLYP) functionals are used.

The chapter is organized as follows: first we discuss the constraints imposed by the molecular symmetry on the orientation of the electric and magnetic dipole transition moments, then after describing the computational procedure the results are presented and discussed. Finally, the chapter is summarized with some concluding remarks.

5.2 Theory

As shown in chapter 2, section 2.1.4, in achiral molecules the EDTMs and the MDTMs of a given mode i are perpendicular, i.e. $\xi(i) = 90°$, whereas in chiral molecules they are usually not , i.e. $\xi(i) \neq 90°$.

Symmetry constraints can impose further restrictions on the orientation of the EDTMs and MDTMs. Thus, in chiral molecules that have symmetry only certain values are permitted for the angles $\xi(i)$. Chiral molecules belong to point groups that have only proper rotation axes: C_1, C_n, D_n (with $n \geq 2$), T, O and I. As an example, we will consider the case of a molecule with C_2 symmetry. Group theory states that a matrix element of the form $\langle\psi_a|\hat{O}|\psi_b\rangle$ is zero unless the integrand transforms as the totally symmetric representation of the molecular

point group:

$$\Gamma(\psi_a) \times \Gamma(\hat{O}) \times \Gamma(\psi_b) = A \tag{5.1}$$

For the matrix elements associated with the EDTM and MDTM of a given mode i, see Eq. (2.143), Eq. (5.1) is written:

$$\Gamma(0) \times \Gamma(\hat{O}) \times \Gamma(1) = A \tag{5.2}$$

where the operator $\hat{O}$ is either $(\vec{\mu}_E)_k$ or $(\vec{\mu}_M)_k$ $(k = x, y, z)$.

As can be seen in Eq. (2.7), the components of the electric dipole operator, $\vec{\mu}_E$, transform as the components of the vectors $\vec{r}_a$ and $\vec{R}_\lambda$ (as translations x, y, z in the character tables). From Eq. (2.8), the components of the magnetic dipole operator, $\vec{\mu}_M$ transform as the components of angular momentum (as rotations R_x, R_y, R_z in the character tables).

For C_2 symmetry the z Cartesian components of both $\vec{\mu}_E$ and $\vec{\mu}_M$ have A symmetry, whereas the x and y components have B symmetry. The normal modes of molecules with C_2 symmetry have either A or B symmetry. The harmonic wave function associated to the ground vibrational state, $|0\rangle$, has A symmetry for all modes [22], whereas the harmonic wave function of the first excited vibrational state, $|1\rangle$, of a mode i has the same symmetry as the mode i (either A or B symmetry) [22]. Thus, for modes of A symmetry the left term of Eq. (5.2) becomes:

$$\Gamma(0) \times \Gamma(\hat{O}) \times \Gamma(1) = A \times \Gamma(\hat{O}) \times A = A \times \Gamma(\hat{O}) \tag{5.3}$$

In order to have $A \times \Gamma(\hat{O}) = A$ in Eq. (5.3) and thus, non-zero electric and magnetic dipole transition moments, $\Gamma(\hat{O})$ is necessarily A. Thus, in modes of A symmetry only the z Cartesian components of both transition dipole moments are non-zero. As a result, the transition dipole moments $\vec{E}_{01}(i)$ and $\vec{M}_{10}(i)$ are either parallel $\xi(i) = 0°$ or antiparallel $\xi(i) = 180°$.

For modes of B-symmetry, we have:

$$\Gamma(0) \times \Gamma(\hat{O}) \times \Gamma(1) = A \times \Gamma(\hat{O}) \times B = B \times \Gamma(\hat{O}) \tag{5.4}$$

In order to have $B \times \Gamma(\hat{O}) = A$ in Eq. (5.4) and thus non-zero electric and magnetic dipole transition moments, $\Gamma(\hat{O})$ is necessarily B. This means that in modes of B symmetry the x and y Cartesian components of both transition dipole moments are non-zero. Since the two transition dipole moments can have any orientation in the xy plane, there are no symmetry restrictions on the values taken by the $\xi(i)$ angles in the modes of B symmetry. Using the character tables, similar conclusions can easily be obtained for all the point groups.

Finally, we note that in the chiral molecules without symmetry there are no restrictions on the orientations of the EDTMs and MDTMs. As a result the two

transition dipole moments can have any orientation with respect to each other. This means that in chiral molecules without symmetry the angles ξ can take any value between 0° and 180°.

5.3 Method

In the first part of the study presented in this chapter the values of the ξ angles are investigated. Thus, 27 chiral molecules ranging from very small molecules (5 atoms) to relatively large molecules (48 atoms) have been considered. The distributions of the values of the angles ξ of each molecule are analyzed by calculating the arithmetic means, $\bar{\xi}$, and the standard deviations, $\sigma(\xi)$. Since in most VCD studies in the literature only the finger print region is considered (the frequency interval between 800 and 1800 cm^{-1}), we have analyzed the distribution of the ξ angles of all normal modes and also of only the finger print modes.

In the second part of the study presented in this chapter, we investigate the differences between the values of the ξ angles calculated with the BP86 and OLYP functionals. For a consistent evaluation of these differences a one-to-one mapping between the BP86 and OLYP modes of each molecule is established first by calculating overlaps of normal modes. The normal modes overlaps (Ω) are calculated according to the procedure described in chapter 4 section 4.3.

As expected, the modes obtained with the two functionals, although very similar, are not identical. Thus, for all the molecules considered, an overlap of at least 0.90 has been calculated for more than 90% of the BP86 and OLYP modes; the remaining 10 percent show overlaps of at least 0.7.

The modes of one functional can be obtained as linear combination of the modes of the other functional:

$$\vec{V}(i,\mathrm{BP86}) = \sum_j \Omega(i,j)\vec{U}(j,\mathrm{OLYP}) \tag{5.5}$$

where $\vec{V}(i,\mathrm{BP86})$ and $\vec{U}(j,\mathrm{OLYP})$ are the $3N$-dimensional vectors defined in Eq. (4.3) associated to the BP86 i^{th} and OLYP j^{th} normal modes, respectively. The expansion coefficients, $\Omega(i,j)$, are the normal modes overlaps, and are calculated according to Eq. (4.5). Since the modes calculated with a given functional are orthogonal, we have:

$$\sum_j \Omega^2(i,j) = 1 \tag{5.6}$$

Thus, an overlap of 0.90 between a BP86 and an OLYP mode means that the two modes differ by 20%, whereas an overlap of 0.70 means that the two modes differ

by 51%. As a result, when analyzing the differences, $\Delta\xi$, between the angles ξ calculated with the two functionals, we have considered only the BP86–OLYP mode pairs with overlaps of at least 90°. The distributions of the values of $\Delta\xi$ are analyzed by calculating for each molecule the arithmetic mean, $\overline{\Delta\xi}$, of all the $\Delta\xi$,

$$\overline{\Delta\xi} = \frac{1}{N_{\Delta\xi}} \sum_{a=1}^{N_{\Delta\xi}} \Delta\xi_a, \quad \Delta\xi_a = \xi_a(BP86) - \xi_a(OLYP). \tag{5.7}$$

the largest $\Delta\xi$, $\Delta\xi_{max}$,

$$\Delta\xi_{max} = max(|\Delta\xi_a|) \tag{5.8}$$

and the standard deviation of all $\Delta\xi$, $\sigma(\Delta\xi)$,

$$\sigma(\Delta\xi) = \frac{1}{N_{\Delta\xi}} \left[\sum_{a=1}^{N_{\Delta\xi}} \left(\overline{\Delta\xi} - \Delta\xi_a\right)^2 \right]^{\frac{1}{2}} \tag{5.9}$$

In Eqs. (5.7), (5.8) and (5.9) $N_{\Delta\xi}$ is the number of BP86–OLYP normal mode pairs considered for each molecule, which is not always the total number of modes, see below.

The number of BP86-OLYP mode pairs considered, $N_{\Delta\xi}$, is determined as follows. In the first place, as noted above, a pair is not taken into account whenever the overlap $\Omega(a, a)$ is below 0.90. In the second place we have excluded modes with small EDTM or MDTM because we have found that very large $\Delta\xi$ can be encountered when at least one of the transition dipole moments of a normal mode has very small magnitude. As an example, we compare the EDTMs and MDTMs of mode 52 of benzoyl-benzoic acid (BBA) (molecule **21** in Fig. 5.1) calculated with the BP86 and OLYP functionals.

Table 5.1 lists the overlap (Ω) of the BP86 and OLYP modes, the frequency, rotational strengths, the angles ξ, and the Cartesian components of the EDTMs and MDTMs calculated with the two functionals. As can be seen, the BP86 and OLYP modes of pair 52 of BBA have very similar frequencies and normal modes (the normal modes overlap is 0.99). The MDTMs of both functionals have relatively large magnitudes and similar values, their Cartesian components are also very similar. Thus, the direction of the MDTM of mode 52 of BBA was not affected by the change of functional. However, mode 52 of BBA has a very small EDTM (also compared to the rest of BBA modes). Both functionals have predicted for it values that are very close to zero. Due to its small magnitude its direction can be easily perturbed. As can be seen in Table 5.1 this is indeed the case, the BP86 and OLYP Cartesian components of the EDTMs of mode 52 are all small but very different. As a result the BP86 and OLYP ξ angles are

Ω =0.99		$\Delta\xi = 61.81$	
	Freq.	R	ξ
BP86:	1151.54	1.27	49.92
OLYP:	1162.00	-0.97	111.73
$\vec{E}_{01}(i)$	x	y	z
BP86:	-1.74	0.67	-2.29
OLYP:	-3.06	1.51	1.32
$\mathrm{Im}[\vec{M}_{01}(i)]$	x	y	z
BP86:	-14.56	-35.34	-54.57
OLYP:	-12.32	-35.82	-61.13

Table 5.1: Comparison of the frequencies (cm^{-1}), rotational strengths (10^{-44} esu·cm), ξ angle, electric dipole transition moments (10^{-21} esu·cm) and magnetic dipole transition moments (10^{-25} esu·cm) of the normal mode 52 of BBA calculated using the BP86 and OLYP functionals

quite different ($\Delta\xi = 61.81°$). Clearly, the angle ξ of mode 52 of BBA cannot be reliably calculated, and most likely also perturbation due to a solvent would greatly change it. It should therefore be classified as a *non-robust* mode from the outset, and so should all modes with very small EDTM and/or MDTM.

We cannot give an absolute measure, valid for all molecules, to determine what should be considered small in this context. The magnitudes of the total EDTM and MDTM of a normal mode depend on the type of mode and on the number of atoms involved in the normal mode motion, i.e. on the molecule. However, for a given molecule one can easily determine the threshold value for "small". Take the mean values of all EDTMs and of all MDTMs of all modes of that molecule, then the magnitude of a DTM of some mode is classified as "small" if it is less than 10% of the mean value.

The total number of BP86–OLYP mode pairs considered after removal of these small-DTM modes, $N_{\Delta\xi}$, is listed for each molecule in Tables 5.3 and 5.4 (compare to total number of modes in Table 5.2). $N_{\Delta\xi}$ is typically some 10% smaller than the total number of modes.

As in the previous chapters, all calculations (geometry optimization and IR/VCD calculations) were performed using the ADF program package [24–26]. The BP86 and OLYP functionals and the TZP basis set were used in all the calculations. The geometries have been optimized separately for each choice of

functional using the optimizer described in reference [44]. Very tight convergence criteria have been applied for the geometry optimization (10^{-6} Hartree for the energy and 10^{-4} Hartree/Ångström for the gradients).

5.4 Results and Discussions

Figure 5.1 shows schematic representations of all 27 test molecules we have considered for this study.

5.4.1 Characterization of robust modes

We will first consider possible differences between the finger print modes and the rest of the modes. We have analyzed the distributions of the angles ξ of all the normal modes, $\bar{\xi}_{all}$ and $\sigma(\xi_{all})$, and also of the finger print modes, $\bar{\xi}_{fp}$ and $\sigma(\xi_{fp})$, of each molecule. Table 5.2 lists the arithmetic means $\bar{\xi}_{all}$ and $\bar{\xi}_{fp}$, the standard deviations $\sigma(\xi_{all})$ and $\sigma(\xi_{fp})$, the total number of normal modes, and also the number of finger print modes for all 27 molecules.

As can be seen in Table 5.2, roughly half of the normal modes of a given molecule are in the finger print region. The only exception is molecule **3** which has only 2 out of its 9 modes in the finger print region. There are no significant differences between the distribution of ξ of all normal modes and the distribution of ξ of the finger print modes. The values of the ξ angles are distributed equally around 90°, the arithmetic means $\bar{\xi}_{all}$ and $\bar{\xi}_{fp}$ have both values that are very close to 90°. There are very few cases where the averages $\bar{\xi}_{all}$ and/or $\bar{\xi}_{fp}$ deviate from 90° by more than 5° ($\bar{\xi}_{all} = 96.75$ and $\bar{\xi}_{fp} = 99.20$ for **17**, $\bar{\xi}_{fp} = 100.54$ for **9**, and $\bar{\xi}_{fp} = 84.75$ for **10**). So even if in chiral molecules the ξ angles of individual modes may differ greatly from 90°, as is apparent from the large spread $\sigma(\xi)$ in the ξ values that exists for some molecules, e.g. 63° and 75° for molecules 1 and 2, the spread is obviously practically symmetrical around 90°. This statement remains true also when applied to just the finger print modes, although in that case the deviation of $\bar{\xi}_{fp}$ from 90° tends to be a bit larger, cf. the largest deviations quoted above. Similarly, only small variations are observed when comparing the standard deviations $\sigma(\xi_{all})$ and $\sigma(\xi_{fp})$. The differences between $\sigma(\xi_{all})$ and $\sigma(\xi_{fp})$ are less than 5° for 21 of the 27 molecules, less than 9° for the next 5 molecules and 14.66° for molecule **3** (which has only 2 finger print modes). We can therefore conclude that there do not seem to be systematic differences between the finger print modes and the other ones, which justifies the use of the former for the analysis of the VCD spectra. Our differentiation between robust and non-robust

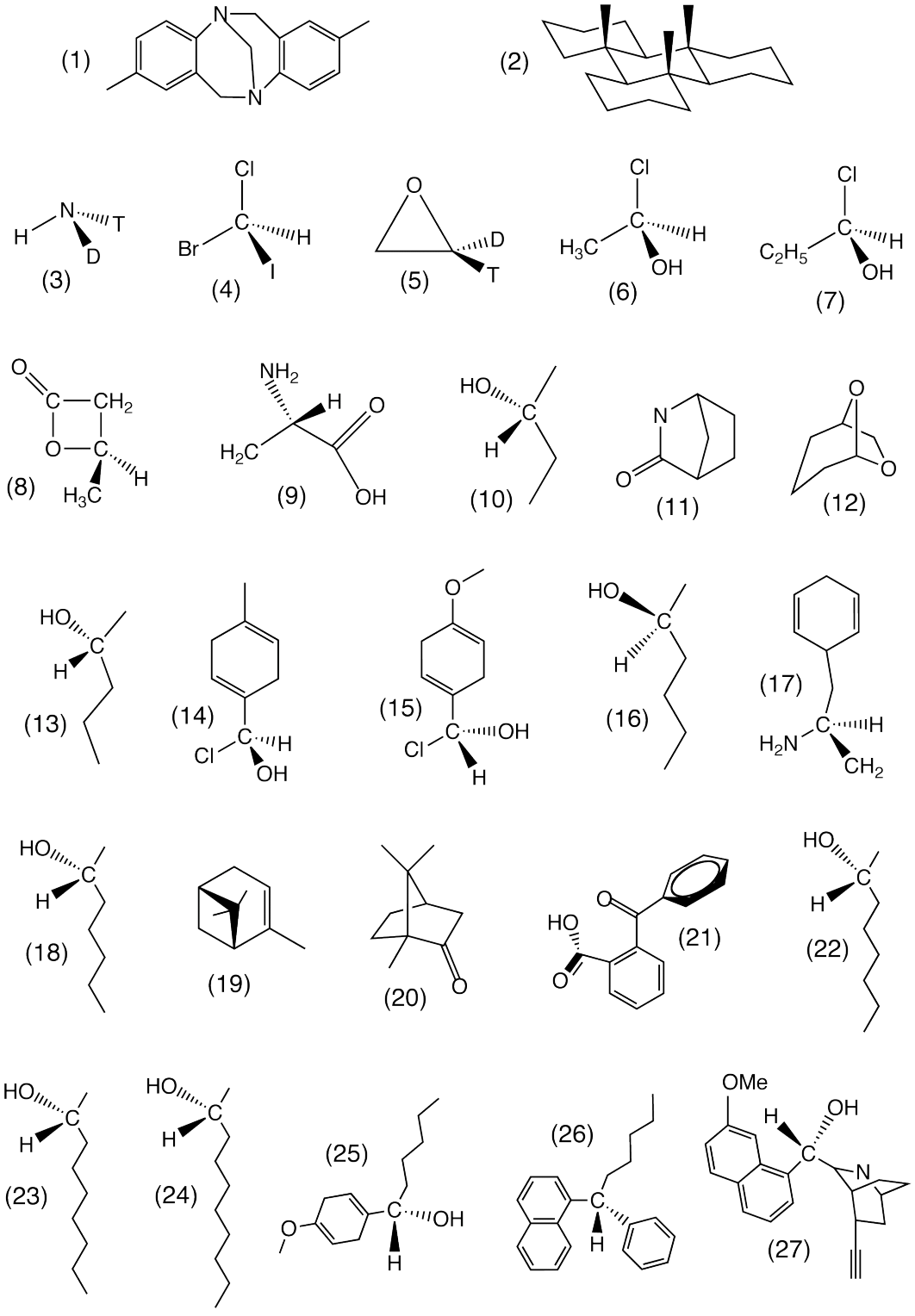

Figure 5.1: Schematic representation of the 27 molecules analyzed.

	All modes			Finger print modes		
Molecule	N	$\bar{\xi}$	$\sigma(\xi)$	N_{fp}	$\bar{\xi}$	$\sigma(\xi)$
1	105	93.16	62.66	54	92.82	65.65
2	138	90.40	75.47	78	89.71	77.64
3	6	92.86	23.55	3	93.36	12.15
4	9	90.46	20.10	2	90.70	5.44
5	15	91.31	14.86	8	93.94	18.36
6	21	92.94	29.59	10	93.47	36.95
7	30	93.37	30.71	14	94.00	39.23
8	30	90.67	31.03	15	92.37	36.86
9	33	90.92	30.39	15	100.54	31.92
10	39	88.26	16.69	19	84.75	15.18
11	45	90.43	32.52	25	89.14	36.78
12	48	89.71	36.40	28	91.18	39.08
13	48	92.42	20.59	25	89.61	24.21
14	51	91.56	32.12	25	91.95	30.37
15	54	89.04	29.67	25	87.31	32.44
16	57	91.57	22.04	29	90.67	28.15
17	63	96.75	27.67	34	99.20	29.01
18	66	89.08	25.33	34	87.22	31.83
19	72	90.21	29.77	37	92.85	33.80
20	75	87.36	28.77	39	89.53	30.57
21	74	86.78	20.03	35	89.78	11.90
22	75	91.42	23.41	38	89.44	26.57
23	84	91.59	25.50	42	91.41	29.56
24	93	92.21	23.26	47	91.04	27.36
25	99	89.04	17.80	49	87.96	19.26
26	132	89.93	24.73	66	88.03	24.26
27	132	89.52	12.49	64	88.33	9.94

Table 5.2: Statistics of the angles ξ. $\bar{\xi}$ is the arithmetic mean and $\sigma(\xi)$ is the standard deviation of the angles ξ of a given molecule. The total number of modes (N) and the number of the finger print modes (N_{fp}) of each molecule are also given.

modes, see below, will be applicable to all the modes, including the finger print modes.

In order to make the distinction between robust and non-robust modes we consider the typical magnitude of a change in the angle ξ caused by change of

	All modes				Finger print modes			
Molecule	$N_{\Delta\xi}$	$\overline{\Delta\xi}$	$\Delta\xi_{max}$	$\sigma(\Delta\xi)$	$N_{\Delta\xi_{fp}}$	$\overline{\Delta\xi}$	$\Delta\xi_{max}$	$\sigma(\Delta\xi)$
3	6	0.25	6.29	3.74	3	0.23	0.34	0.13
4	9	-4.12	3.48	6.26	2	-0.12	1.29	1.41
5	14	1.35	9.66	3.41	7	2.47	9.66	4.14
6	21	0.43	6.27	3.96	10	0.91	4.68	2.02
7	24	1.09	24.77	9.42	13	-1.02	16.67	10.38
8	30	1.27	23.82	7.41	15	-0.46	10.73	5.69
9	33	0.54	19.92	6.22	15	-1.12	3.77	3.64
10	35	-0.38	4.28	2.86	19	-0.33	4.28	3.38
11	42	-0.89	13.40	7.22	25	-0.88	13.40	7.03
12	42	0.78	18.02	7.10	26	-0.06	18.02	6.31
13	45	0.57	20.83	6.31	25	1.03	20.83	7.15
14	41	-0.81	26.89	7.05	25	-0.56	26.89	7.63
15	49	0.08	25.24	9.31	23	-0.36	25.24	9.92
16	53	0.54	27.10	5.93	28	-0.05	9.81	5.74
17	57	1.44	27.46	7.30	31	1.20	27.46	7.54
18	54	0.35	19.18	6.20	30	1.04	19.18	6.45
19	58	-1.10	21.03	7.68	27	-0.80	21.03	7.79
20	63	0.28	27.82	8.51	38	1.15	27.82	9.15
21	58	-0.10	15.94	5.66	29	0.29	15.94	4.08
22	68	0.65	23.46	6.41	35	1.73	13.95	4.22
23	63	-0.54	12.74	6.45	33	-0.28	12.74	7.92
24	79	-0.38	11.72	6.19	44	0.75	11.72	5.25
25	91	0.21	23.65	6.26	46	0.58	16.66	5.72
26	111	0.13	26.05	6.77	55	0.46	26.05	7.21
27	110	-0.16	20.71	5.43	56	-0.25	16.08	4.45

Table 5.3: Statistics of $\Delta\xi$ (the difference between the BP86 and OLYP ξ angles). $\overline{\Delta\xi}$ is the arithmetic mean of all $\Delta\xi$ of a molecule, $\Delta\xi_{max}$ is the maximum $\Delta\xi$ for a molecule, $\sigma(\Delta\xi)$ is the standard deviation of the $\Delta\xi$ of a molecule. The total number of modes considered ($N_{\Delta\xi}$) and the number of the finger print modes among $N_{\Delta\xi}$ ($N_{\Delta\xi_{fp}}$) for each molecule are also given.

functional. We investigate the characteristics of the distribution of $\Delta\xi$ values, and the differences between the angles ξ calculated with BP86 and OLYP. This investigation is carried out for the modes that remain after we have excluded the ones that can be characterized as non-robust from the outset on the basis of the smallness of the EDTM and/or the MDTM, see Section 5.3. In addition, the

Molecule	$N_{\Delta\xi}$	N_{sign}	$\Delta\xi > 20°$	$\Delta\xi > 25°$	$\Delta\xi > 30°$
3	6	0	0	0	0
4	9	2	0	0	0
5	14	2	0	0	0
6	21	0	0	0	0
7	24	0	2	1	0
8	30	2	2	0	0
9	33	1	0	0	0
10	35	3	0	0	0
11	42	0	2	0	0
12	42	5	0	0	0
13	45	5	1	0	0
14	41	1	1	1	0
15	49	6	3	1	0
16	53	5	2	1	0
17	57	3	1	1	0
18	54	9	1	0	0
19	58	9	2	0	0
20	63	4	1	1	0
21	58	6	0	0	0
22	68	12	2	0	0
23	63	12	2	1	0
24	79	13	1	0	0
25	91	10	2	0	0
26	111	10	3	1	0
27	109	8	2	0	0

Table 5.4: The number of BP86-OLYP normal modes pairs considered ($N_{\Delta\xi}$) and the number of modes that have changed sign upon changing the functional (N_{sign}). The last three columns give the numbers of BP86-OLYP modes pairs with $\Delta\xi$ larger or equal to 20°, 25°, 30°, respectively.

modes that mix are excluded. (This is not a criterium for non-robustness that can be used when just a single calculation with a chosen functional is performed; see the comments on how to deal with this phenomenon of mode mixing at the end of the paper.) Table 5.3 gives for each molecule the number of BP86–OLYP mode pairs considered, $N_{\Delta\xi}$, the arithmetic mean of the values of $\Delta\xi$, $\overline{\Delta\xi}$, the absolute value of the largest $\Delta\xi$, $\Delta\xi_{max}$, and the standard deviations of the distributions of $\Delta\xi$, $\sigma(\Delta\xi)$ (see Section 5.3 for more details).

As before, no significant differences between the data associated with all normal modes and the data associated with the finger print modes are observed. The averages $\overline{\Delta\xi}$ are close to zero. This means that the two functionals do not have a systematic difference. The standard deviations $\sigma(\Delta\xi)$ are almost all below 8°, there are only three outliers at 8.5°, 9.3° and 9.4°. Since about 95% of a Gaussian distribution are within 2 standard deviations from the mean, one should expect that 95% of the modes will have a $\Delta\xi$ smaller than 16°. Looking at the values of $\Delta\xi_{max}$ in Table 5.3, it may be noted that indeed there are some molecules with $\Delta\xi_{max} > 20°$, but $\Delta\xi$ is never larger than 30°; the largest value, $\Delta\xi_{max} = 27.82°$, is exhibited by molecule **7**. To gain a more thorough understanding of the data in Table 5.3, we have listed in Table 5.4 the number of BP86–OLYP mode pairs with rotational strengths of different signs (N_{sign}) and the number of mode pairs with $\Delta\xi$ larger than 20°, 25° and 30°, respectively. As can be seen in Table 5.4 there are very few pairs of modes (≤ 3 for each molecule) with $\Delta\xi > 20°$ and even fewer (≤ 1 for each molecule) with $\Delta\xi > 25°$; as noted, none of the molecules has a $\Delta\xi$ larger than 30°. It is also important to note that, in general, the number of modes of a molecule whose rotational strength changes sign, N_{sign}, is much larger than the number of modes with a large $\Delta\xi(> 20°)$. This clearly shows that the rotational strengths of many modes with relatively small $\Delta\xi$ still change sign, so they must have had ξ angles close to 90°. Of course those modes are most susceptible to change sign. It should also be realized that a large $\Delta\xi$ does not imply a change of ξ across 90°, if the few mode pairs with $\Delta\xi > 20°$ happened to have ξ angles very different from 90°. An example in this regard is molecule **7** which has one mode with $\Delta\xi > 20°$ and one mode with $\Delta\xi > 25°$, but none of the modes of **7** have changed sign when going from BP86 to OLYP ($N_{sign} = 0$).

We have also verified whether a correlation between the value of ξ and the magnitude of the $\Delta\xi$ exists. However, no consistent pattern was observed, i.e. a large $\Delta\xi$ can be exhibited equally well by modes with ξ that are close to or far from 90°. Since $\Delta\xi > 20°$ do occasionally occur, we conclude that a safe criterium would be that *robust* modes should have angles ξ that differ from 90° by at least 30°.

5.4.2 Molecules with symmetry

Troger's base and D_3−anti-trans–anti-trans–anti-trans–perhydrotriphenylene (molecules **1** and **2** in Fig. 5.1 and Table 5.2), have C_2 and D_3 symmetry, respectively. As shown in section 5.2, many of the modes of chiral molecules with symmetry have angles ξ that are far from 90° (e.g. 0° or 180°). As a result, the molecules **1** and **2** have very large standard deviations, i.e $\sigma(\xi_{all}) = 62.66°$

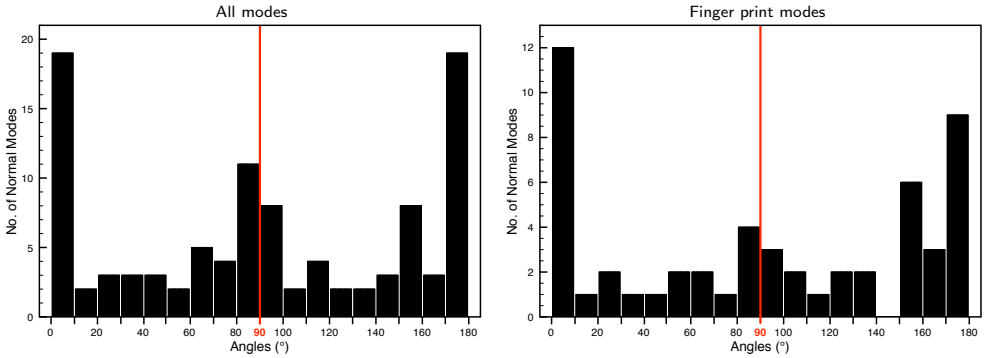

Figure 5.2: Distribution of the values of the ξ angles of molecule **1** (C_2 symmetry). The left panel shows the distribution of all normal modes (ξ_{all}). The right panel shows the distribution of the finger print modes (ξ_{fp}).

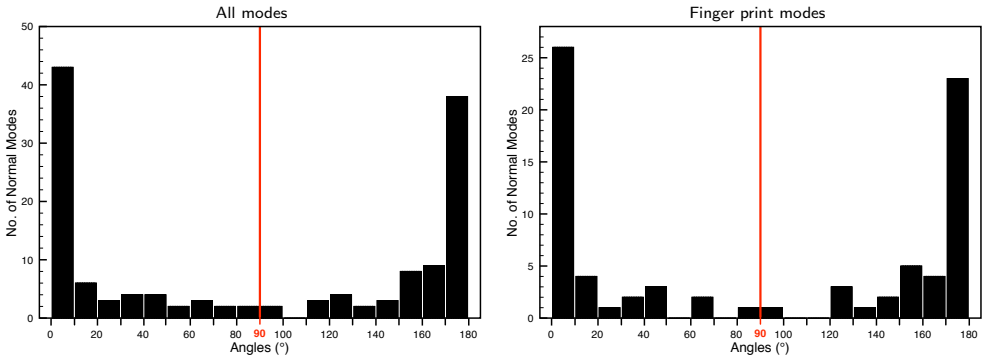

Figure 5.3: Distribution of the values of the ξ angles of molecule **2** (D_3 symmetry). The left panel shows the distribution of all normal modes (ξ_{all}). The right panel shows the distribution of the finger print modes (ξ_{fp}).

and $\sigma(\xi_{fp}) = 65.65°$ for **1**, and $\sigma(\xi_{all}) = 75.47°$ and $\sigma(\xi_{fp}) = 77.64$ for **2**. These values are clearly much larger than the values of the standard deviation of the molecules without symmetry—which are smaller than 40° and mostly between 20° and 30° (see Table 5.2).

The distribution of the angles ξ_{all} and ξ_{fp} of molecules **1** and **2** are shown in Figs. 5.2 and 5.3, respectively. In Figs. 5.2 and 5.3 the horizontal axis represents the angle interval from 0° to 180° (divided into 10° intervals), whereas the vertical axis gives the number of normal modes in a given 10° interval. As can be seen, the distributions of the angles ξ of both molecules have a concave shape with peaks at 0° and 180°. Because they have many modes with angles ξ far from 90°, the molecules **1** and **2** have potentially many robust modes, a fair number of those 0° and 180° modes being expected to be also sufficiently intense.

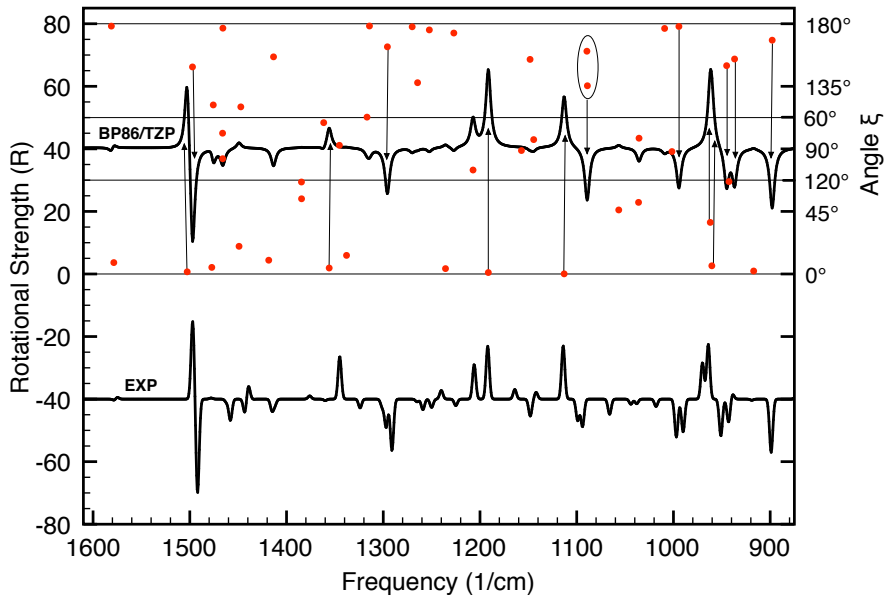

Figure 5.4: Comparison of calculated (BP86/TZP) and experimental (EXP) VCD spectra of molecule **1** (C_2 symmetry).

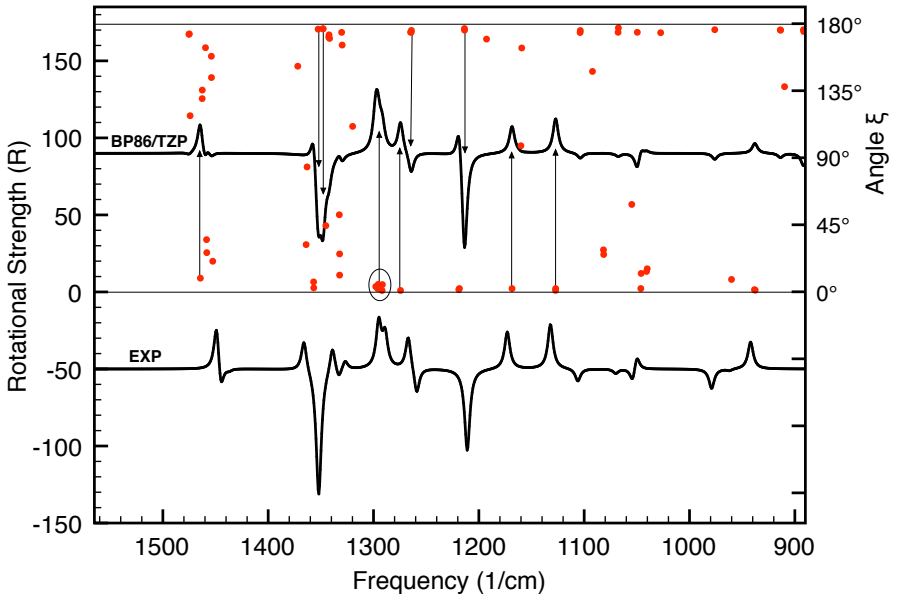

Figure 5.5: Comparison of calculated (BP86/TZP) and experimental (EXP) VCD spectra of molecule **2** (D_3 symmetry).

Figures 5.4 and 5.5 show a comparison of the calculated and experimental VCD spectra of **1** and **2**, respectively. The calculated spectra were obtained from BP86/TZP ADF gas phase calculations on the isolated molecules, the experimental spectra were obtained by Lorentzian broadening of the experimental VCD intensities reported by Stephens et all. [54, 82]. The dots plotted in Figs. 5.4 and 5.5 on top of the VCD spectra indicate the magnitude of the ξ angles of the modes in the calculated spectra. The baseline of the calculated spectra is the 90° line, the Y-coordinate of each dot gives the magnitude of each ξ angle (see the vertical right axis in Figs. 5.4 and 5.5), while the X-coordinate gives the frequency of the mode. The *robust* modes (the modes with significant VCD intensities and values of their ξ angle that differ from 90° by more than 30° degrees) are marked with arrows in Figs. 5.4 and 5.5.

As can be seen, there is a very good agreement between the calculated and experimental VCD spectra of both molecules. All the features that stand out in the VCD spectra of **1** and **2** are associated with *robust* modes. As a matter of fact, even the non-robust modes usually also have the same sign as in the experiment. Finally, we note that the molecules **1** and **2** are very rigid, and as shown in references [54] and [82] these molecules practically have a single conformation populated. Thus, the experimental VCD spectra of both molecules are indeed for the same conformation for which the calculations are performed. We can therefore conclude that in cases like the present ones—rigid molecules with symmetry and therefore many robust modes—it is easy to obtain reliable predictions of the ACs using VCD.

5.4.3 Molecules without symmetry

The rest of the molecules in Fig. 5.1 and Table 5.2 (**3** to **27**) have no symmetry. As already mentioned, the molecules without symmetry have much smaller spread of the ξ values, i.e. $\sigma(\xi)$, around 90° than the molecules with symmetry. Thus, the largest value of $\sigma(\xi_{all})$ is exhibited by **12**, $\sigma(\xi_{all}) = 36.40$, whereas the smallest value is exhibited by **27**, $\sigma(\xi_{all}) = 12.49$ (see Table 5.2). In the case of $\sigma(\xi_{fp})$, the largest value is exhibited by **7**, $\sigma(\xi_{all}) = 39.23$, whereas the smallest value is exhibited by **4**, $\sigma(\xi_{fp}) = 5.44$ (**4** has only 2 finger print modes, both of them with ξ close to 90°).

Approximately 65% of the elements of a Gaussian distribution are situated within one standard deviation from the mean. Because the values of $\sigma(\xi_{all})$ and $\sigma(\xi_{fp})$ of the molecules without symmetry are relatively small, many of the modes of these molecules have ξ that are close to 90° (the approximate mean value), and therefore are *non-robust* modes.

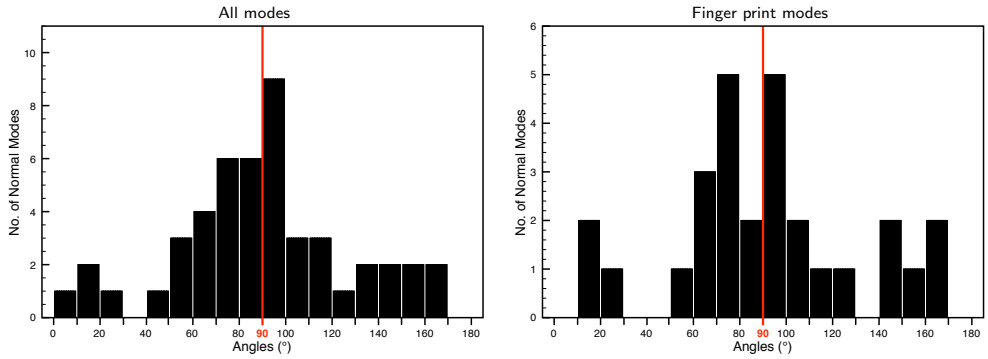

Figure 5.6: Distribution of the values of the ξ angles of molecule **12** (no symmetry). The left panel shows the distribution of all normal modes (ξ_{all}). The right panel shows the distribution of the finger print modes (ξ_{fp}).

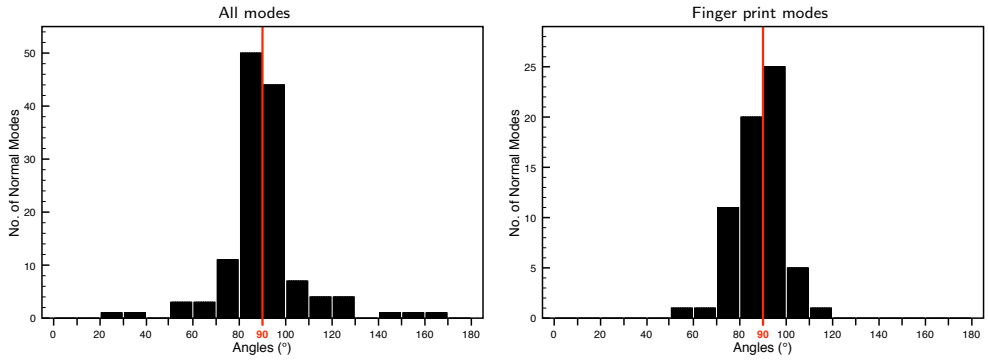

Figure 5.7: Distribution of the values of the ξ angles of molecule **27** (no symmetry). The left panel shows the distribution of all normal modes (ξ_{all}). The right panel shows the distribution of the finger print modes (ξ_{fp}).

As suggested by the data in Table 5.2, all the molecules without symmetry have very similar gaussian-like ξ distributions that are centered approximately on the 90° value. The distribution of the ξ angles of the molecules without symmetry have been carefully investigated. For brevity we will discuss here only two suggestive examples. Figures 5.6 and 5.7 show the distributions of ξ_{all} and ξ_{fp} of molecules **12** and **27**, respectively.

Among the molecules without symmetry, molecule **12** has some of the largest standard deviations $\sigma(\xi_{all})$ and $\sigma(\xi_{fp})$, i.e 39.08° and 36.40°, respectively. As a result, relatively many of its normal modes have ξ angles that are far from 90° (see Fig 5.6) and therefore are classified as *robust*. Furthermore, **12** is a rigid molecule that does not have much conformational freedom, therefore the experimental VCD spectra (measured in inert solvents such as CCl_4 and CS_2) do

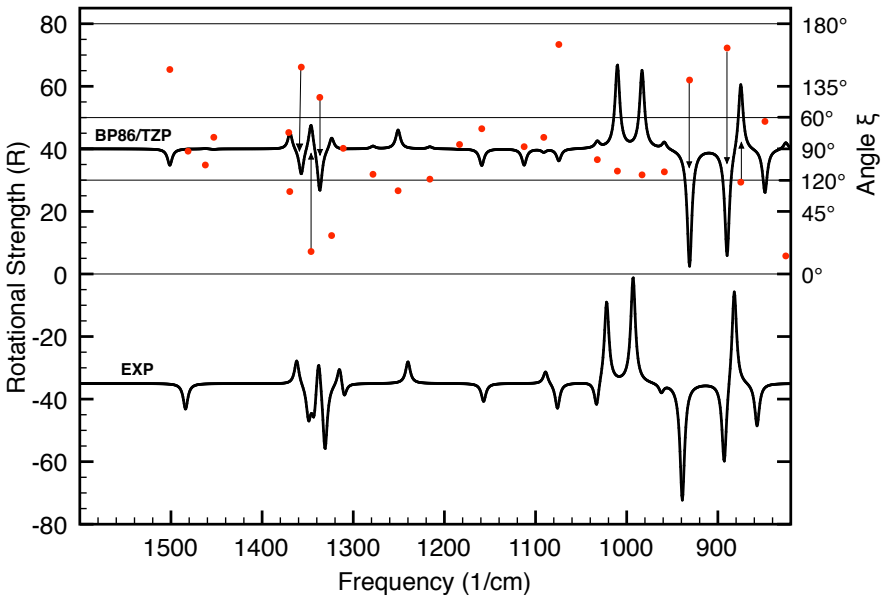

Figure 5.8: Comparison of calculated (BP86/TZP) and experimental (EXP) VCD spectra of molecule **12** (no symmetry).

relate to a single conformer.

Figure 5.8 shows the calculated and experimental VCD spectra of **12**. The calculated spectrum was obtained from a BP86/TZP ADF gas phase calculation on an isolated molecule, the experimental spectrum was obtained by Lorentzian broadening of the experimental VCD intensities measured in CS_2 solvent reported in reference [92]. As before, the dots indicate the values of angles ξ of the modes in the calculated spectra, while the arrows indicate the *robust* modes. The calculated VCD spectrum reproduces very well the experimental one. The *robust* modes all agree in sign and intensity with the experimental spectrum. This allows to conclude that the prediction of the AC of **12** using the comparison of VCD calculation and experiment is a very reliable one. As a matter of fact, also many of the *non-robust* modes in the calculated VCD spectrum of **12** have the correct sign, notably the three intense modes around 850, 980 and 1010 cm^{-1}. This gives the total calculated spectrum a superficially very similar appearance as the experimental one. We should however caution that for the non-robust modes the agreement is somewhat accidental in view of the possible effects of error sources (functional, solvent effects). Indeed, there are also non-robust modes that do have different signs in calculation and experiment, e.g. at 1030 cm^{-1} and 1090 cm^{-1}, the calculated one at 1110 cm^{-1} being not visible in experiment. It only

so happens in this molecule that the intense non-robust modes are in agreement with experiment, while the ones that are not have small intensities and therefore are not conspicuous.

It may happen that a molecule has only few robust modes. Consider molecule **27**, which (together with molecule **26**) has the highest number of modes of our set of molecules (132) but which has some of the smallest values for the standard deviations $\sigma(\xi_{all})$ and $\sigma(\xi_{fp})$. As can be seen in Fig. 5.7, most of its modes have angles ξ that are very close to 90° and as a result are *non-robust*. Molecule **27** has only nine robust modes. In fact, only two of the nine robust modes are in the finger print region. Thus, if these robust modes are intense, and are not sensitive to the conformation, they may be used for determination of the AC. (**27** is a very flexible molecule that may adopt many different conformations in solution, but this is a complication we do not address here). However, one should expect to obtain a sub-optimal agreement between the calculated and experimental VCD spectra for molecule **27**.

Finally, we note that the large difference between the standard deviations of the ξ angles of molecules **12** and **27** can be qualitatively understood by looking at their geometrical structures. As shown in section 2.1.4, in achiral molecules the EDTM and MDTM associated with the normal modes are always perpendicular ($\xi = 90°$). Molecule **27** is a very large molecule with many of its normal modes being localized on only one of the four different groups attached to the chiral carbon. Some of these modes, especially the ones localized far from the chiral center, are very similar (almost identical) to the modes of the free group on which they are localized. This is also the case for the APTs and AATs of the atoms that are far from the chiral center (see chapter 4 and [93]). Thus, when such modes are localized on achiral groups, their ξ angles should have values that deviate only slightly from 90°. Molecule **12** on the other hand, is a very small and compact molecule that has two chiral centers. Due to its compactness, molecule **12** has no parts that can behave like isolated achiral molecules and therefore its ξ angles deviate significantly from 90°.

5.5 Summary and conclusions

The sign of the rotational strength of a given mode in a VCD spectrum is determined by the angle ξ made by the EDTM and MDTM of that mode. The modes with $\xi < 90°$ have positive VCD signals ($R > 0$), whereas the modes with $\xi > 90°$ have negative VCD intensities ($R < 0$). However, when ξ is close to 90°, even the smallest perturbation can change ξ across 90° and thus induce a

sign change. Since as shown in chapter 4 (cases **C** and **D**) rotational strengths can have large magnitudes also when ξ is very close to 90°, variation of ξ by few degrees can significantly modify the shape of the VCD spectra if the angle change occurs across 90°. An important perturbation at the experimental side is the influence of the solvent, perturbations at the computational side are change of functional or basis set.

In this chapter we have investigated the distributions of the values of the angles ξ and their dependence on the exchange-correlation functional, using a test group of 27 molecules. The results of the analysis presented in this chapter have validated further the conclusions drawn in chapter 4. That is, the modes in a VCD spectrum can be classified as *robust* and *non-robust*. The *robust* modes have rotational strengths with characteristic sign that is not sensitive to small perturbations (either of computational or experimental nature) and as a result should be correctly predicted by calculations. On the other hand, the signs of the rotational strengths of *non-robust* modes can be changed even by the smallest perturbation and as a result should not be trusted.

The analysis of the differences between BP86 and OLYP calculations has shown that:

1) The differences, $\Delta\xi$, between the ξ angles of BP86–OLYP pairs of modes with $\Omega \geq 0.90$ and large EDTMs and MDTMs were always smaller than 30°. It is therefore clear that the two functionals will not predict different signs for the rotational strengths of modes with angles ξ that differs from 90 by more than 30° (unless perhaps if it mixes strongly with another mode, i.e. when $\Omega \leq 0.90$).

2) When a mode has very small EDTM and/or MDTM, a very large $\Delta\xi$ can be encountered ($\Delta\xi > 70°$ are not unusual). Thus, quite often the BP86 and OLYP Rs have different signs.

Based on 1) and 2) we conclude that the *robust* modes are characterized by angles ξ that differ from 90° by at least 30° and by rotational strengths of significant magnitude, i.e. large EDTMs and MDTMs. *Non-robust* modes are characterized by ξ angles that are close to 90° and/or by rotational strengths of small magnitude, i.e. small EDTM and/or MDTM, where we have defined "small" earlier.

Since the sign of the rotational strengths of *non-robust* modes are not reliable, only *robust* modes should be considered when determining the absolute configuration of chiral molecules using VCD. Thus, in order to have reliable VCD prediction it is required that the modes that are used to determine the AC of the molecule are *robust*. On the other hand, sign differences between experimental and calculated VCD signals should be of no concern if the signals are associated with *non-robust* modes.

Although this definition of *robustness* is very useful, it is not a 100% guarantee that a robust mode will not change sign. Occasionally, sign differences are encountered also for modes which are *robust* according to the above criteria. We have already mentioned that robust modes may mix strongly with another mode with similar frequency in response to the small change induced by the change of functional (cf. BP86–OLYP mode pairs with overlaps smaller than 0.90, i.e $\Omega \leq 0.90$). The "mixed" modes differ significantly from the initial modes (an overlap of 0.70 means that the two modes differ by 51%) and as a result they often have rotational strengths that are very different from the rotational strengths of the initial modes. Such situations also occur in experiment, i.e. the small perturbations present in experiment (e.g solvent effects) may cause normal modes with similar frequencies to mix (such an example will be discussed in the next chapter). Typically less than 10% of the modes of a molecule are in this category. In case different signs are encountered for one or a few of the *robust* modes, the strategy to be followed is to examine whether the cause could be mixing of modes due to a perturbation. From the displacement vectors of the calculated mode (e.g., do they involve atoms that may participate in hydrogen bonding with the solvent?) and taking into account the type of solvent used, one may detect if there is the possibility of mixing of modes by solvent effects. In the calculations, one can check on proximity of other modes. So if in the comparison of calculation to experiment the signs of most of the robust modes agree, but a few anomalous sign changes are observed, one may assume this is caused by mode mixing. This can then be confirmed by performing a second calculation where the interaction is explicitly specified (e.g calculation for the hydrogen-bonded complex) or a computational perturbation (different functional) is applied.

The analysis of the distribution of the values of the ξ angles has shown that there is a significant difference between the distributions of the molecules with and without symmetry. Due to constraints imposed by symmetry on the orientation of the EDTMs and MDTMs, the distribution of the values of the angles ξ has a concave shape with peaks at 0° and 180°. The values of the angles ξ of the chiral molecules without symmetry on the other hand, have gaussian-type distributions that have a maximum at about 90°. This means that molecules with symmetry have many more *robust* modes than the molecules without symmetry. Thus, under normal conditions it is to be expected that better agreement will be obtained between calculated and experimental VCD spectra for molecules with symmetry. As proven by the multitude of literature reports, good agreement between calculation and experiment may also be obtained for molecules without symmetry. As we have shown in this study, this happens when the molecules have enough *robust* modes in the finger print region. However, it is important to realize that

there are also cases when the molecules without symmetry have very few *robust* modes in the finger print region (e.g. **27** has only two *robust* modes in the finger print region). In such chases a sub-optimal agreement between calculation and experiments is usually obtained.

We should caution, however, against overinterpreting the "prediction" of VCD for such molecules if based on a superficial comparison of the experimental and calculated spectra. Only *robust* modes should be considered when determining the absolute configuration of chiral molecules using VCD. We advocate that codes that calculate vibrational rotational strengths should output the angles ξ and the magnitude of the EDTMs and MDTMs. This will enable to assign the *robustness* of each mode in the calculated VCD spectrum which will greatly aid the interpretation of the differences between the calculation and experiment.